

Implementing Adaptive Ensemble Biomolecular Applications at Scale

Vivek Balasubramanian*, Travis Jensen†, Matteo Turilli*, Peter Kasson‡, Michael Shirts†, Shantenu Jha*§

*Department of ECE, Rutgers University

†Department of ChBE, University of Colorado Boulder

‡Biomedical Engineering, University of Virginia

§Brookhaven National Laboratory

Abstract—Many scientific problems require multiple distinct computational tasks to be executed in order to achieve a desired solution. Novel approaches focus on leveraging intermediate data to adapt the application to study larger problems, longer time scales and to engineer better fidelity in the modeling of complex phenomena. In this paper, we describe types of application adaptivity in such applications, develop abstractions to specify application adaptivity, and challenges in implementing them in software tools. We describe the design and enhancement of Ensemble Toolkit to support adaptivity, characterize the adaptivity overhead, validate the implementation of two exemplar molecular dynamics algorithms: expanded ensemble and markov state modeling, and analyze the results of running the expanded ensemble algorithm at production scale. We discuss novel computational capabilities enabled by abstractions for adaptive ensemble applications and the scientific advantages arising thereof.

Index Terms—Adaptivity, Ensemble Applications

I. INTRODUCTION

Current computational methods for solving scientific problems in bio-molecular science are at or near their scaling limits. Advances in high performance computing (HPC) infrastructures occur by scaling out their systems to include more compute resources as opposed to scaling up existing resources. Consequently, a number of these methods, called *ensemble based methods*, in bio-molecular science have been developed to take advantage of the growing number of compute resources where multiple tasks are executed on these compute resources in parallel. Although these methods may suffice for existing problems, studying larger systems for longer durations will require sophistication in these algorithms. Specifically, studying larger physical systems will not only require tools that can support 100x - 1000x greater degrees of parallelism but also 1) exploration of "adaptive" applications, and 2) automation to encode and execute complex algorithm logic. In order to enable encoding the logic and encourage development of novel algorithms, there is also a need for abstractions to hide runtime complexities and expose components necessary for application creation while minimizing the learning cost. This paper aims to define a simple high-level formalism to capture adaptive applications and analyze performance considerations associated with adaptivity to enable scalable adaptive applications.

We define adaptivity as the capability to change, based on current information available, one or more attributes that influence execution performance or domain specific parameter(s).

It is important to identify and differentiate adaptivity at the various levels of executing an application on a HPC system. Adaptivity may occur at three levels: within an individual task, over multiple tasks, and during the mapping of tasks to resources. Within an individual task, the execution kernel may be capable of using information local to the task to make adaptive execution decisions, some examples of which we discuss in §II. Adaptivity may occur over a collection of multiple tasks wherein decisions are made using information from multiple tasks, examples from the molecular dynamics domain serve science drivers for our work and are discussed in §III. Lastly, adaptivity may exist across tasks of an application and the available resources where information from both the application as well as the available resources is used to decide the mapping of the tasks to the resources [1]. In this paper, we focus on the adaptivity across the multiple tasks of an application, which we refer to as *application adaptivity*.

Adaptivity and automation are critical requirements for scaling to bigger systems and longer simulation durations in many scientific applications. The application cannot be simply enumerated *a priori* but depends upon intermediate results and adaptive methods to improve sampling quality, sampling rate or steer execution towards interesting phase space or parameters. To achieve scalability and efficiency, such adaptivity cannot be performed via user intervention and hence automation of the control logic and execution is important.

To guide the design and implementation of capabilities to execute ensemble- based biomolecular applications in a scalable and adaptive manner, we identify two adaptive applications used in production. Although each of these biomolecular applications have distinct coordination and communication patterns among their ensemble members and execution requirements, they are united by their need for adaptive execution of multiple concurrent tasks. This paper makes the following contributions:

- analyzes the steps to execute an adaptive application and identifies different types of adaptivity
- enhances an ensemble execution system (EnTK) with adaptive capabilities and characterizes the cost of supporting diverse adaptive features
- demonstrates the capability to execute novel adaptive applications at scale and validates the scientific results from these applications

To the best of our knowledge, this is the first that multiple adaptive ensemble applications have been implemented using a common conceptual and implementation framework. This paper focusses on biomolecular applications, but the results apply to ensemble-based adaptive applications in domains, such as climate, uncertainty quantification and seismic physics.

The paper is organized as follows: Section II describes existing solutions and their limitations in their ability to support adaptive applications. Section III presents two science drivers that motivate the need for large-scale adaptive biomolecular simulations. We describe adaptive execution, their different types and challenges in supporting adaptivity in section IV. In section V, we describe the design and implementation of the EnTK, and the enhancements made to address the challenges of adaptivity. In section VI, we characterize the overheads in EnTK as a function of the adaptivity types, validate the implementation of the science drivers using EnTK, and discuss the results of executing the expanded ensemble application at production scale.

II. RELATED WORK

Molecular dynamics (MD) simulations provide quantitative and qualitative information about the structure and stability of molecular systems, and the interactions among them. Novel computer architectures specialized for MD enable brute force simulations in the order of milliseconds [2], [3]. Nonetheless, higher availability in general purpose machines and the need to investigate biological processes taking place in the time scales ranging from milliseconds to seconds are critical motivations for alternative approaches to the sampling problem.

Ensemble-based simulation methods such as replica exchange [4]–[7], meta-dynamics [8], [9], swarm-of-trajectories [10], [11], and Markov state modeling [12], [13] can be performed on general-purpose machines including clouds, clusters and supercomputers. Ensemble-based simulation methods are more powerful when they do not simply explore configuration space independently, but exchange information to analyze intermediate data and make adaptive decisions about the configuration of ongoing simulations. Adaptive decisions enable better sampling of conformational space and characterization of complex conformational dynamics.

MD software packages like Amber [14], Gromacs [15] and NAMD [16] offer ensemble and adaptive capabilities to support multiple independent MD simulations, multi-dimensional replica exchange, steered MD, adaptive biasing or meta-dynamics. However, these capabilities are limited and many adaptive biomolecular applications use these MD packages solely as simulation kernels [17]–[20]. Further, these MD packages use MPI to communicate between ensembles, incurring communication overheads and failures at large scale.

Executing adaptive biomolecular applications on HPC systems requires specific knowledge of resource, data and execution management. Several middleware frameworks [21] have been developed to abstract some of these details from the user. For example, gSOAP [22] enables web services for HPC

applications, while Ninf-G [23] and OmniRPC [24] support distributed programming via a client/server architecture. These solutions provide methods to launch application tasks on remote machines but leave the details of task scheduling, resource and data management, and fault tolerance to the user.

Multiple workflow systems aim to support execution of adaptive biomolecular applications on HPC systems. Ref. [25] lists several workflow systems supporting adaptation to computational resources, task and data configurations, and domain data. However, most of these systems enable adaptation to support fault tolerance instead of application steering on the base of the preliminary results of ongoing simulations. For example, in Ref. [26], authors discuss enhancement of Kepler [27] to re-execute failed tasks or execute new tasks based on intermediate results. Taverna was extended to support task fail-and-retry mechanisms via loop constructs [28]. Pegasus [29] was used within the Stampede framework [30] to predict failures and enable runtime refinement of tasks.

Domain-specific projects have also been developed to run adaptive biomolecular applications. Copernicus [31] is a domain-specific workflow system to perform Markov state modeling on trajectories. Although the workflow system provides an interactive and customized interface to the domain scientist, it requires users to manage resource selection, access and acquisition; bootstrapping of the master/client infrastructure needed to execute the tasks of the workflow; and setting up the execution environment, including making available the MD libraries required by the tasks.

Specifying the application, including its adaptivity, in the user libraries of the HPC or services offered by the middleware bounds the capability to the specific HPC and middleware respectively [32]. In contrast, specification directly in the application code enables flexibility on runtime behavior and portability. The flexibility enables runtime adaptivity allowing applications to be tunable to changes in the execution environment and steer the execution by modifications to the application workflow [32].

In this paper, we develop abstractions for the user to specify MD applications capable of runtime adaptivity. These abstractions enable and accelerate distributed collaborative efforts towards explorative scientific methodologies, via rapid reuse and improvement of existing software frameworks.

III. SCIENCE DRIVERS

Traditionally, bio-molecular algorithms have been formulated as static and fully defined workflows. A number of powerful algorithms have emerged that require both the management of large ensembles of simulations and have adaptive features. We discuss two representative but important algorithms.

A. Expanded Ensemble

Metadynamics [33]–[35] and expanded ensemble (EE) dynamics [36]–[44] are another class of algorithms, where, similar to replica exchange, individual simulations jump between simulation conditions. In EE dynamics, the simulation states take one of N discrete states of interest, whereas in meta-dynamics,

the simulation states are described by one or more continuous variables. In contrast to replica exchange, the change of simulation conditions of each simulation is not directly coupled together, but instead each simulation explores states independently. Additional weights are required to force the simulations to visit desired distributions in simulation condition space space, which usually involves sampling in all the simulation conditions. These weights are learned adaptively using a variety of schemes [37], [40], [41].

Since the movement between state spaces is essentially diffusive, the larger the simulation state spaces that are used, the more sampling is slowed down. This can be handled using “multiple walker” approaches, with more than one simulation exploring the same state space [45]–[47].

As discussed above, there are a number of adaptive choices in the methods for collectively building up the weights [37], [40], [41]. Another choice of adaptivity includes partitioning the simulation condition range of individual simulations (smaller partitions decrease diffusive behavior [46], but the “best” partitions to spend time sampling may not be known until after simulation). Additionally, EE and meta-dynamics are far more adaptable to changes in the resources available than replica exchange, as the number of simulations can dynamically increase or decrease, and any choice of adaptivity can be much more asynchronous, as the need for collective exchange at set checkpoints required for replica exchange is eliminated.

In this paper, we implement the EE algorithm as a workflow consisting of concurrent, iterative ensemble members that exchange data at regular intervals. In our workflow, each ensemble member consists of two types of tasks: simulation and analysis. The simulation tasks generate MD trajectory data while the analysis tasks uses this MD trajectory data, both current and historical, from all the ensemble members to generate simulation condition weights for the next iteration of simulation in its own ensemble member. In this method, every analysis task operates on the current snapshot of the total global data. Note that the analysis uses any and all data available at a point and does not explicitly “wait” for any data from other ensemble members. Figure 1 is a representation of this implementation. We choose to implement EE rather than expanded ensemble meta-dynamics because of the greater range of simulation adaptivity that can be explored with EE.

B. Markov state modeling

Markov state modeling is another important class of simulation algorithms for determining kinetics of molecular models. Using an assumption of separation of time scales of molecular motion, the rates of first-order kinetic processes are learned adaptively. In a typical Markov State Model simulation, a large ensemble of simulations, typically tens or hundreds of thousands, are run from different starting points, and similar configurations are clustered as states. The rates of transitions between these states are estimated by observing which the entire kinetic behavior can then be inferred even though individual simulations perform no more than one state transition. However, the choice of where new simulations are initiated to

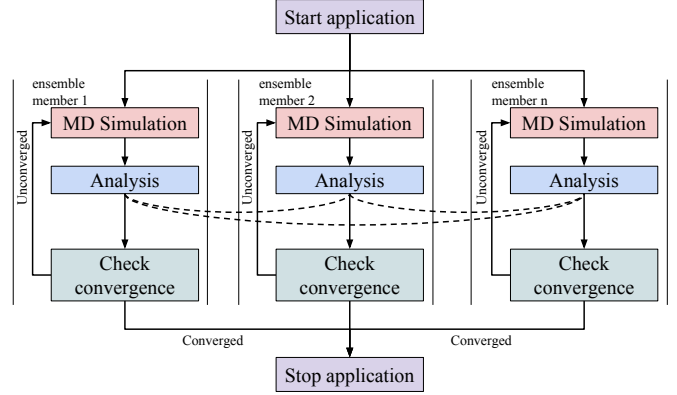


Fig. 1: Workflow of the EE science driver consists of multiple independent ensemble members. The analysis operates on both current and historic data from all the ensemble members. At the end of the analysis, the workflow terminates if convergence is reached in any ensemble member, else the next simulation is triggered.

best refine the definition of the states, improve the statistics of the rate constants, and how to discover new simulation states requires a range of analyses of previous methods, making the entire algorithm highly adaptive.

Markov State Models provide an attractive way to encode dynamic processes such as protein folding into a set of metastable states and transitions between them. In computing these models from simulation trajectories, the metastable state definitions and the transition probabilities have to be inferred. It has previously been shown both theoretically [48], [49] that “adaptive sampling” can lead to more efficient MSM construction as follows: provisional models are constructed using intermediate simulation results, and these models are used to direct the placement of further simulation trajectories. Here, we have applied adaptive sampling prospectively to the folding of the Fip35 WW domain as a moderately challenging but tractable proof of concept. This workflow consists of an iterative pipeline in two stages: ensemble simulation and MSM construction to determine optimal placement of further simulations. The pipeline is iterated until convergence of the resulting Markov State Model.

We implement MSM workflow as an ensemble of simulation tasks and an analysis task. The workflow is executed iteratively till sufficient amount of MD trajectory data is generated before moving to analysis. The analysis task, operates over the entire data to generate a new set of simulation configurations. These configurations are used in the simulation tasks of the next iteration. It is important to note two points about this workflow: there exist two iterations: *local*, that generates the necessary amount of data and *global*, that improves the sampling of the state space. Figure 2 is a representation of this workflow.

a) *Other example of adaptive bio-molecular algorithms*:: Replica exchange or parallel tempering [45], [50]–[55] is one of the most common methods to improve the amount of configurational sampling per unit computational time of large-scale molecular simulations. In replica exchange, a series of simulations running under different simulation conditions (such as different temperatures or pressures) are loosely coupled to

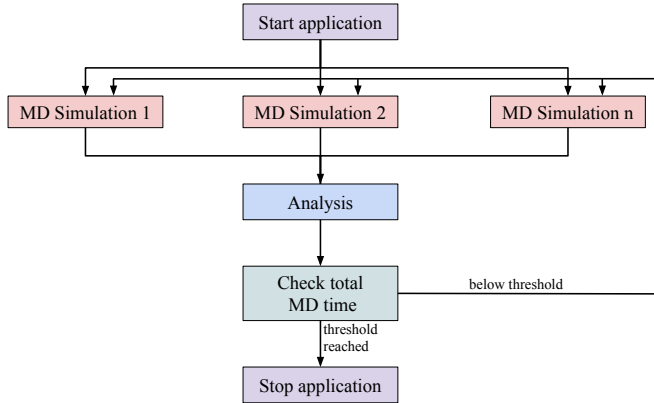


Fig. 2: Workflow of the MSM science driver consists of an iterations of the simulation and analysis tasks. There exists a synchronization barrier between the simulation and analysis tasks. The analysis task is only triggered after sufficient simulation data is available. The analysis operates on this data to produce a new set of configurations for the next iteration of simulation tasks. Both the amount of sufficient simulation data and number of configurations generated by the analysis are parameters that may change during runtime.

gether, exchanging configurations stochastically in a way that preserves the correct probability distribution for each simulation condition. Such simulations can achieve sampling of configurations faster than running the simulations independently. For example, since kinetics are typically faster at higher temperature, replica exchange allows all of the simulations to spend some time at higher temperatures and visit more configurations.

However, as new replica-exchange based algorithms are developed that sample over three or four different simulation conditions [56], or even over multiple molecular models [57]–[59], the number of simulations in the ensemble increases to the power of number of simulation variables. In order to manage this size and complexity, adaptive choices must be made about how to switch between ensemble members and which of all the possible simulations should be run at any given time.

Adaptive decisions make it possible to traverse the high-dimension conformational space through the states most efficiently so they can move back and forth. In multidimensional space, it allows one to prune out states that are not important to maximizing the flow to important states. This can be achieved by adjusting (i) the spacing between replicas (are they closer or further in temperature) adaptively, and/or (ii) adding or subtracting replicas or activating or deactivating replicas, and/or (iii) adjusting which replicas exchange with others, and/or (iv) adding or subtracting dimensions, has the potential to increase the exchange rate and thereby the quality of simulations. In spite of these advantages however, most replica-exchange simulations are currently formulated to be non-adaptive, viz., the simulations and how they couple are statically determined. This is primarily due to the high barrier and complexity of managing multiple concurrent and coupled replica (ensemble-members) in traditional HPC environments.

IV. APPLICATION ADAPTIVITY

In this section, we introduce the terminology we will use across the paper to discuss about adaptivity, adaptive appli-

cations, and their support. We decompose the execution of adaptive applications into four operations, describing the abstractions they require. Further, we discuss different modes of adaptivity, explaining the challenges they pose.

A. Working Definitions

Terms like “task”, “application”, “graph”, “workload” and “adaptivity” are often overloaded in literature. Thus, we define the terminology used in this paper:

- **Task** is a generalized term for a stand-alone process that has well defined input, output, termination criteria, and dedicated resources. Specifically, a task is used to represent an independent simulation or data processing analysis, running on one or more cores of a high-performance computing (HPC) machine.
- **Application** is the end-to-end workflow that encodes a science problem in terms of multiple tasks executing independent simulations, data processing kernels, and domain specific data analysis.
- **Task graph (TG)** represents all tasks in an application alongside the interdependencies that determine their execution order. Scientific applications contain unique tasks where the execution is known to begin and do not consist of cycles. The TG of such applications can be described as a directed acyclic graph (DAG) where the vertices represent the tasks and edges represent the interdependencies.
- **Workload** refers to a set of tasks whose dependencies have been satisfied and are ready to be executed. Workloads can be subsets of tasks of a TG. Further, the “load” in workload is a reference to a measure of the computational requirements of each individual task; this is particularly relevant when the tasks are heterogeneous.
- **Application Adaptivity** is defined as modifying the TG of an application based on the intermediate data generated at runtime.

B. Adaptive Execution

Our analysis of adaptive ensemble applications (henceforth called ‘applications’) suggests that the exact TG of applications is not known prior to execution and may change depending on intermediate runtime results. Execution of such applications can be decomposed into four operations as represented in Figure 3: (a) The application is created by encoding the known portions of its TG; (b) the TG is traversed to identify tasks ready for execution in accordance to their dependencies; (c) tasks are executed on the compute resource; and (d) notification of a completed task (control-flow) or generation of intermediate data (data-flow) is used to evaluate and execute adaptations to the TG.

Operations (b)–(d) are repeated till the TG is completely evaluated and all its tasks are executed. We call this sequence of operations an Adaptivity Loop and we use it to distinguish between adaptive and predefined applications. In the former, the application “learns” its future TG based on the execution of its current TG; in the latter, the TG is fully known and only operations (a)–(c) are necessary.

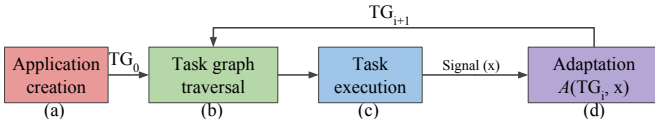


Fig. 3: **Adaptivity Loop**: Sequence of operations in executing an adaptive application.

Encoding of adaptive applications requires two sets of abstractions to describe: (i) the application TG; and (ii) the adaptive methods (A) that, upon receiving a signal x , operate on a TG TG_i . The former set of abstractions are required for creating the application, i.e., operation (a), while the latter set of abstractions are required to adapt the TG, i.e., operation (d).

C. Adaptivity types

The Adaptation operation (Fig. 3d) of the adaptivity loop consists of applying an adaptive method on the TG of the application. We represent the TG as a DAG, $TG = [V, E]$, with a set of vertices V , denoting the tasks of the application and attributes of the tasks (such as executable, required resources, and required data), and a set of directed edges E , denoting dependencies between the tasks. For an application with $TG = [V, E]$, there exist four parameters that may change during execution: (i) set of vertices; (ii) set of edges; (iii) size of the vertex set; and (iv) size of the edge set. We analyzed the 16 permutations of these parameters and identified 3 that are valid and unique. The remaining permutations represent conditions that are either not possible to achieve or combinations of the 3 valid permutations.

a) *Task-count adaptivity*:: We define a method A_{tc} (operator) as a task-count adaptive method if, on receiving a signal x , the method performs the following adaptation (operation) on the TG (operand):

$$TG_{i+1} = A_{tc}(TG_i, x) \\ \implies \text{size}(V_i) \neq \text{size}(V_{i+1}) \wedge \text{size}(E_i) \neq \text{size}(E_{i+1})$$

where $TG_i = [V_i, E_i]$ and $TG_{i+1} = [V_{i+1}, E_{i+1}]$. Task-count adaptivity refers to adaptation in the number of tasks in the TG, i.e., the adaptive method operates on a TG to produce a new TG such that at least one vertex and one edge is added or removed to/from TG_i to produce TG_{i+1} .

b) *Task-order adaptivity*:: We define a method A_{to} as a task-order adaptive method if, on a signal x , the method performs the following adaptation:

$$TG_{i+1} = A_{to}(TG_i, x) \implies E_i \neq E_{i+1} \wedge V_i = V_{i+1}$$

where $TG_i = [V_i, E_i]$ and $TG_{i+1} = [V_{i+1}, E_{i+1}]$. Task-order adaptivity refers to adaptation in the dependency order among tasks, i.e., the adaptive method operates on a TG to produce a new TG such that the vertices are unchanged but at least one of the edges between vertices is different between TG_i and TG_{i+1} .

c) *Task-attribute adaptivity*:: We define a method A_{ta} as a task-attribute adaptive method if, on a signal x , the method performs the following adaptation:

Science Driver	Requirement	Adaptivity type
Expanded Ensemble	<ul style="list-style-type: none"> dynamically add new simulations, remove executing simulations dynamically determine when to terminate dynamically vary seed values for simulations and data for analysis 	<ul style="list-style-type: none"> task count adaptivity task order adaptivity task attribute adaptivity
MSM	<ul style="list-style-type: none"> dynamically determined number of simulations dynamically determine when to terminate 	<ul style="list-style-type: none"> task count adaptivity task order adaptivity

TABLE I: Mapping of requirements from science drivers to adaptivity modes

$$TG_{i+1} = A_{ta}(TG_i, x) \\ \implies V_i \neq V_{i+1} \wedge \text{size}(V_i) = \text{size}(V_{i+1}) \wedge E_i = E_{i+1}$$

where $TG_i = [V_i, E_i]$ and $TG_{i+1} = [V_{i+1}, E_{i+1}]$. Task-attribute adaptivity refers to adaptations in the attributes of tasks, i.e., the adaptive method operates on a TG to produce a new TG such that the edges and the number of vertices are unchanged but the attributes of at least one vertex is different between TG_i and TG_{i+1} .

The adaptive requirements of two algorithms of the science drivers presented in §III are listed in Table I and mapped to the three types of adaptivity discussed above.

Using the notation presented above, we can express the two algorithms as:

- Expanded Ensemble (EE). Consider N ensemble members executing independent of each other in multiple iterations. We represent the ensemble members at each iteration as a task graph TG. The adaptations of TG in the algorithm is represented as:

parallel_for [1 : N]:

while (condition on x):

$TG = A_{ta}(A_{to}(A_{tc}(TG)))$

- MSM: We represent the application task graph during each iteration as TG and its adaptations between iterations as:

while (condition on x):

$TG = A_{ta}(A_{tc}(TG))$

D. Challenges in encoding adaptive applications

Adaptive capabilities can be beneficial to domain science applications but supporting them comes with three main challenges.

The first challenges lies in the expressibility of adaptive applications. Composition of adaptive applications requires APIs that enable the expression of the initial state of the

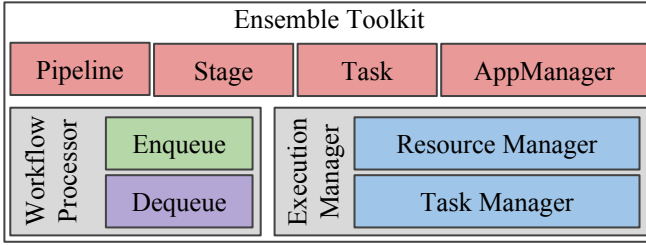


Fig. 4: Components and sub-components of EnTK depicted with their responsibilities in supporting the four operations of the adaptation loop.

application and specification of methods that capture how the application adapts to intermediate data. The former translates to a description of the application TG while the latter specifies adaptive methods that adapt this TG.

The second challenge is in determining when the adaptation is instantiated. The adaptation is described at the end of the execution of a task wherein a new TG is generated. Different strategies can be employed in the instantiation of the adaptation [60].

The third challenge lies in implementation of the adaptation of the application during runtime. We divide this challenge into three parts: (i) propagation of adapted TG to all components; (ii) consistency of the state of the TG among different components; and (iii) minimal overhead of performing adaptive operations compared to the execution duration of the tasks.

V. ENSEMBLE TOOLKIT

We discussed the design, implementation and performance of EnTK in earlier work [61], [62]. EnTK decouples the description of ensemble-based applications from their execution by separating three concerns: specification of tasks and resource requirements; resource selection and acquisition; and task execution management. EnTK sits between the user and the HPC system, abstracting resource management and execution management complexities from the user.

EnTK exposes an API for composing ensemble-based applications and supports the execution of up to $O(10^4)$ concurrent tasks on heterogeneous HPC systems, abstracting complexity of task execution and resource management from the user. Currently, EnTK supports predefined applications, i.e., application for which the user knows the complete TG prior to execution. In contrast, the science drivers discussed in this paper require support of adaptive applications while preserving the existing capabilities of usability, functionality and performance of EnTK. Thus, we discuss how EnTK has been enhanced to support the three types of adaptivity discussed in §IV-C.

A. Architecture

Figure 4 offers a schematic representation of EnTK. EnTK exposes an API with three objects (Pipeline, Stage, and Task), a user-facing component called ‘AppManager’, a workflow management component called ‘Workflow Processor’, and a workload management component called ‘Execution Manager’.

We use tasks, stages, and pipelines to describe the TG of an application:

- **Task:** abstraction of a computational task consisting of the specification of the executable, software environment, resource and data requirement.
- **Stage:** set of tasks without mutual dependencies that, therefore, can be concurrently executed.
- **Pipeline:** sequence of stages such that any stage i can be executed only after stage $i-1$.

Applications are described as a set or sequence of pipelines, where each pipeline is a list of stages, and each stage is a set of tasks. A set of pipelines executes concurrently whereas a sequence of pipelines executes sequentially. All the stages of each pipeline execute sequentially, and all the tasks of each stage execute concurrently. In this way, we describe an application in terms of the concurrency and sequentiality of tasks, without requiring explicit specifications of dependencies.

The description of an application is passed to the AppManager, alongside an indication of the resource for its execution. The AppManager holds the global state of the application, instantiates other components and sub-components, and sets up message queues for the communication among them.

The Workflow Processor component creates a copy of the application description, and tags the tasks that are ready for execution. Executable tasks are enqueued and completed tasks are dequeued via the Enqueue and Dequeue subcomponents.

The Execution Manager component enables the acquisition of resources via the Resource Manager sub-component. Once acquired, the sets of tasks are obtained by the Task Manager sub-component via the message queues. These tasks are executed on the acquired resources and, once completed, are transferred back to the Workflow Processor via message queues with the respective return codes. Both the sub-components, Resource Manager and Task Manager, use a runtime system (RTS) to enable the acquisition of resources and execution of tasks.

EnTK can be configured to be coupled with different runtime systems. Along with the generality of the Task object, EnTK ensures capability to support different execution kernels, with and without adaptivity, and extensibility to runtime systems that support resource adaptivity.

B. Implementation

EnTK is implemented in Python, uses the RabbitMQ message queuing system [63] and the RADICAL-Pilot (RP) [64], [65] RTS. All EnTK components are implemented as processes, and all subcomponents as threads. AppManager is the master process spawning all the other processes. Tasks, stages and pipelines are implemented as objects, copied among processes and threads via queues and transactions. Synchronization among processes is achieved by message-passing via queues.

RabbitMQ offers several benefits: (i) producers and consumers do not need to be topology-aware because they interact only with the server; (ii) messages are stored in the server and can be recovered upon failure of EnTK components; (iii) messages can be pushed and pulled asynchronously because data can be buffered by the server upon production; and (iv) supports up to at least up to $O(10^6)$ tasks.

EnTK uses RADICAL Pilot, a pilot system, as the RTS. Pilot systems enable the submission of container jobs to the resource manager of an HPC system. Once scheduled, the container job is used to execute the application’s tasks without requiring for each task to be queued on the HPC system. RP does not attempt to ‘game’ the resource manager of the HPC system: Once queued, the resources are managed according to the system’s policies.

C. Support for Adaptive Execution

In §IV-D, we described challenges for adaptive applications: expressibility, instantiation and implementation of adaptivity. The architecture described above is not sufficient to support adaptive applications where the TG may undergo adaptations at runtime. We enhanced EnTK to address these challenges.

We added to EnTK the capability of specifying post-execution properties for stages and pipelines. These properties require the specification of three functions: one function to evaluate a boolean condition over a runtime parameter, and two functions describing the adaptation, depending on the evaluation of the boolean parameter.

Ref. [60] specifies multiple instantiation strategies, viz., forward recovery (abort the old TG and execute a new TG), backward recovery (abort the old TG and execute both the old and a new TG), proceed (continue to run old TG and start a new TG), and transfer (merge the old TG into a new one).

In EnTK, we implement a non-aggressive instantiation strategy, similar to ‘transfer’, where the new TG is created by extending the current TG by means of post-execution properties. The choice of this strategy is based on the current science drivers where tasks that have already executed and tasks that are currently executing are not required to be adapted but all pending tasks may be adapted.

The global state of the application execution is held in the AppManager component and a local copy of is created in the Workflow Processor upon instantiation. The dequeue sub-component of the Workflow Processor acquires a lock over the local copy, invokes the post-execution properties, transmits the changes to the global copy in the AppManager and releases the lock upon receiving an acknowledgment. This mechanism ensures that all TGs are consistent across all components, and requires minimal communication across components.

Pipeline, stage and task descriptions alongside pipeline and stage post-execution properties address the expressibility of adaptivity. The ‘transfer’ strategy is selected to instantiate adaptivity, and the implementation in EnTK ensures consistency and minimal communication in executing adaptive applications.

VI. EXPERIMENTS

We perform three experiments to characterize the overhead of the task-count, task-order, and task-attribute adaptivity as defined in §IV-C. We measure the adaptivity overhead of EnTK as the time taken to adapt the application as specified by the user method. This duration includes the time taken to invoke and to execute the user method. Adaptivity overheads provide estimates of the scale to which EnTK can be used.

We validate the implementation of the two science drivers by comparing their results against reference data. For the EE science driver, we measure the free energy estimate obtained via EE and compare against reference data obtained by executing a single long MD simulation. For the MSM science driver, we compare the mean eigenvalues obtained by the different micro- and macro-states in our experiment against those obtained by the Msmbuilder tool [66] in Ref [67]. Lastly, we perform four production scale experiments to evaluate the results of EE including a single MD simulation, an ensemble of MD simulations, expanded ensemble with local analysis, and expanded ensemble with global analysis.

We use three application kernels in our experiments: stress-ng [68], GROMACS [69], OpenMM [70] and python scripts. We use stress-ng in the characterization experiments as it enables control of the computational duration of a task. We use GROMACS and OpenMM as the simulation kernel for the EE and MSM experiments respectively. We use the configurational sampling of alanine dipeptide molecule for the validation of the MSM implementation. We use the calculation of binding of the cucurbit[7]uril 6-ammonio-1-hexanol host-guest system for the validation and the production scale experiments of the EE implementation. All experiments were executed from the same host virtual machine to the same target HPC system, SuperMIC [71].

A. Characterization of adaptivity overhead

We perform four experiments to characterize the overheads of EnTK and the runtime system (RTS) as a function of the task-count, task-order, and task-attribute adaptivity. We compare these overheads to the the total execution time of all the tasks to assess their overall impact on the application execution. The durations measured in the characterization experiments are:

- **EnTK Setup Overhead:** Time taken to setup the messaging infrastructure, instantiate components and subcomponents, and validate application and resource descriptions.
- **EnTK Tear-Down Overhead:** Time taken to cancel all EnTK components and subcomponents, and shutdown the messaging infrastructure.
- **RTS Tear-Down Overhead:** Time taken by the RTS to cancel its components and to shutdown.
- **RTS Overhead:** Time taken by the RTS to submit and manage the execution of the tasks.
- **EnTK Management Overhead:** Time taken to process the application, translate tasks from and to RTS-specific objects, and communicate pipelines, stages, tasks and control messages.
- **EnTK Adaptivity Overhead:** Time taken by EnTK to adapt the application as specified by the user method. The duration includes both the time taken to invoke and execute the user method.
- **Task Execution Time:** Time taken to run task executables.

In the first experiment (Fig. 5 (a)), we vary the number of decisions taken about task-count adaptation by adding a fixed number of tasks to the application at each decision point. We run three instances of an EnTK application: each instance has

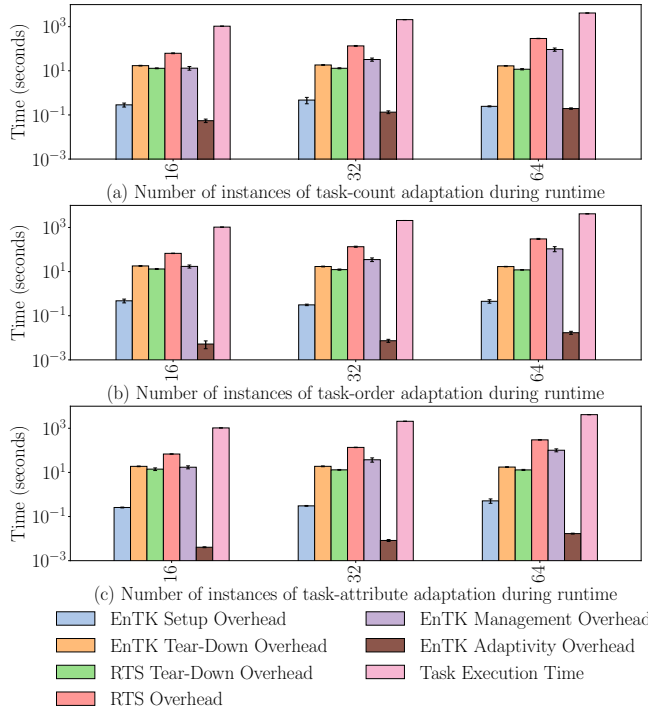


Fig. 5: Overheads and Task Execution Time for a task-count (a), task-order (b), and task-attribute (c) adaptive applications.

1 Pipeline and 16 tasks per Stage, but the number of stages in each instance starts from 1 and increases adaptively to 16, 32, and 64 respectively, by adding 16 tasks at each decision point.

In the second experiment (Fig. 5 (b)), we vary the number of decisions taken about task-order adaptation so that, at each decision point, the tasks of the application are reordered during runtime. We run three instances of an EnTK application: each instance with 1 Pipeline, and 16 tasks per Stage, but the number of stages per Pipeline in each instance varies as 16, 32, and 64. The pending stages are shuffled at the end of the execution of a stage, thereby reordering the tasks of the TG.

In the third experiment (Fig. 5 (c)), we vary the number of decisions taken about task-attribute adaptation by changing the attributes of pending tasks at each decision point during runtime. We run three instances of an EnTK application: each instance with 1 Pipeline, and 16 tasks per Stage, but the number of stages per Pipeline in each instance varies as 16, 32, and 64. At the end of the execution of a stage, an attribute of the tasks in the pending stages are modified during runtime.

In the fourth experiment (Fig. 6), we keep the number of decisions taken about task-count adaptation fixed to 4, but increase the number of tasks adaptively added, from 256 to 512, 1024, and 2048. We test up to 2048 tasks as that is the maximum size of a job allowed by the scheduling policy of SuperMIC. This experiment offers a different perspective of task-count adaptivity, measuring the variation of the overheads as a function of the amount of work done (i.e., number of tasks added) by the adaptive method.

For all the experiments, each task executes the `stress-ng`

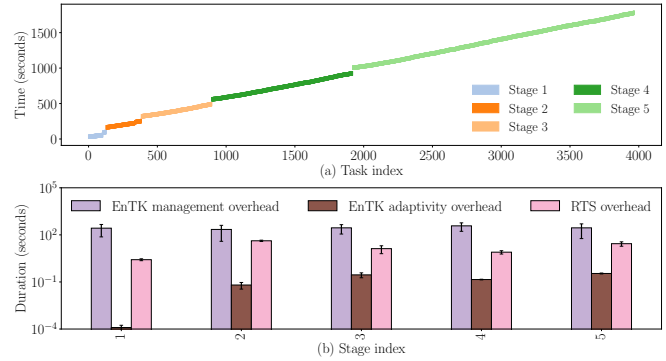


Fig. 6: Execution profile (top) and overheads (bottom) of an adaptive application with varying number of tasks added adaptively.

kernel, running for 60 seconds without moving data. Tasks use 20 cores in the first two experiments, a random number of cores less than 20 in the third, and use 16, 8, 4, 2, and 1 core in each stage of the fourth experiment. The total number of cores acquired for the first three experiments is 340 (320 cores for tasks; 20 cores (1 node) for the RTS) and 2068 (2048 cores for tasks, 20 cores for the RTS) for the fourth experiment.

The execution profile of the first three experiments enables us to characterize the task-count, task-order and task-attribute adaptivity respectively. In Fig. 5, the Setup Overhead of EnTK is ≈ 0.1 s in all the experiments. This behavior is expected as the setup overhead is independent of any application specifics, a factor of the capability of the resources, and one-time cost of EnTK. EnTK is tunable to match resource capability [62].

The EnTK and RTS Tear-Down Overhead are ≈ 18 s and ≈ 13 s respectively. We attribute this duration to the time taken by Python to terminate processes and threads. The Tear-Down overheads can fluctuate within the same Python distribution and HPC system, and vary considerably across different HPC systems and Python distributions.

In Fig. 5, we observe that the RTS overhead increases linearly over the three application instances for all three experiments. We observe similar behavior in each stage in Fig. 6. This is consistent with the expected behavior as an increase in the number of tasks results in an additional cost in their scheduling. The absolute value of the RTS overhead is explained by noticing that: (i) RP initiates communication between the HPC system and a remote database; (ii) RP components communicate via message passing; and (iii) RP depends on the performance of the shared filesystem of the HPC system. EnTK is designed to enable execution of adaptive and predefined applications with different RTS. Thus, a detailed analysis of the RTS overhead is beyond the scope of this paper.

Fig. 5 shows that EnTK Management Overhead increases linearly over the three applications instances in the three experiments. As explained in earlier work [62], this duration is a function of the capabilities of the host machine, and of the number of tasks in the application. Consistently, we observe that the number of tasks increasingly stresses the machine we use for all the experiments, causing the observed linear increase

in the overhead duration. In Fig. 6, we see a similar increase in the EnTK Management Overhead over the different stages due to the increasing number of tasks in each stage. We observe that the absolute value of the EnTK Management Overhead varies depending on whether the RabbitMQ server is instantiated within a Docker container (higher absolute overhead) or in the operating system (lower absolute overhead).

In Fig. 5, EnTK Adaptivity Overhead increases linearly with the number of times the application is adapted. This is explained by noticing that the time required to invoke and execute each adaptive function is constant but that these functions are sequentially invoked and executed an increasing number of times. The absolute value of the EnTK Adaptivity Overhead varies between the three experiments. We attribute this to the variation in the adaptive function specified in the three applications. The adaptive function in the first experiment creates new tasks and adds them to the application, whereas in the second and third experiments, the adaptive method shuffles the remaining stages of tasks and reassigns attributes to the remaining tasks respectively. In Fig. 6, we observe that increasing the number of tasks added up to 2048 does not stress the machine enough to increase the EnTK Adaptivity Overhead.

The Task Execution Time in Fig. 5 increases linearly over the three applications in all three experiments. This is explained by observing that the number of tasks increases across the three applications and that sets of task are executed sequentially in an increasing number of stages of a pipeline. The absolute value of the Task Execution Time is off by $\approx 2\text{-}5\%$ from the expected value. Analysis of the RTS profiles shows that this behavior is due to delays in the scheduling and executing modules of the RTS.

In Fig. 6a, we describe the time-delta execution profile when the number of tasks added adaptively to the application varies. The total execution time is observed to be greater than the expected time of 300 seconds. We attribute this behavior to the scheduling capability of both EnTK and the RTS on the specific HPC system used for the experiment. All the overheads in Fig. 6b are consistent with the understanding derived from the previous experiments.

EnTK takes a step forward in bringing the concepts of application adaptivity to practical use. The characterization experiments describe the EnTK overheads as a function of adaptivity types. The deviation from ideal behavior is explicable, and the causes are candidates for future enhancement.

B. Validation of science driver implementations

We implement the two use cases using the abstractions developed in EnTK. We validate the scientific results obtained from executing these implementations against published references.

1) *Expanded Ensemble*: We implement the EE science driver on XSEDE SuperMIC for an aggregate simulation time of 2270 ns. To validate the process, we carry out a set of simulations of the binding of cucurbit[7]uril (host) to 6-amino-1-hexanol (guest) in explicit solvent for a total of 29.12 ns per ensemble member and compare the final free energy estimate to a reference calculation. Each ensemble member is encoded as a

Pipeline of stages of simulation and analysis tasks in EnTK with each Pipeline using 1 node for 72 hours. With 16 ensemble members for the current physical system, we use 23K core-hours of computation resources.

The expanded ensemble variable is the degree of coupling between the guest and the rest of the system (water and host). As the system explores this coupling variable using EE dynamics, it is able to unbind and bind to the host. The free energy of this process is gradually estimated over the course of the simulation using the Wang-Landau (WL) algorithm [72]. However, we hypothesize we can speed convergence by allowing parallel simulations to share information with each other, and estimate the free energies using the potential energy differences between states with the Multistate Bennett Acceptance Ratio (MBAR) algorithm [73]. Four approaches to communication between the ensemble members are:

- **Method 1:** one continuous simulation (omitting *any* intermediate analysis).
- **Method 2:** multiple parallel simulations without any intermediate analysis.
- **Method 3:** multiple parallel simulations with local analysis, i.e., using current and historical simulation information from only its own ensemble member. This eliminates any effects caused by the intermediate analysis providing a better estimate of the weights than the WL algorithm.
- **Method 4:** multiple parallel simulations with global analysis, i.e., using current and historical simulation information from all ensemble members.

In each method the latter 2/3 of the simulation data available at the time of each analysis is used for free energy estimates using MBAR. In cases where intermediate analysis is used to update the weights the intermediate analysis is always applied at 320 ps intervals.

The reference calculation consisted of four parallel simulations ran with fixed weights, i.e., using a set of estimated weights and not using the Wang-Landau algorithm, ran for 200 ns each. MBAR was used to estimate the free energy for each of these simulations. The reference value is reported as the MBAR estimate of the pooled reference data and its error is reported as the standard deviation of the non-pooled MBAR estimates. Weights used in these fixed weight simulations were estimated by running MBAR on data generated by a 400 ns Wang-Landau algorithm expanded ensemble simulation.

Free energy estimates obtained through each of the four methods are plotted with the reference calculations value in Figure 7. The final estimates of each method agree within error to the reference values, validating that the ensemble based approaches converge the free energy estimate to the true value.

2) *Markov state modeling*: We implement the MSM science driver, described in § III-B for the alanine dipeptide system using the abstractions developed in EnTK. We execute the implementation on XSEDE SuperMIC for an aggregate simulation time of 100ns. Each iteration of the task graph is encoded in EnTK as one Pipeline with 2 stages consisting of 20 simulation tasks and 1 analysis task. Each task uses 1 node with a total walltime of 0.25 hour.

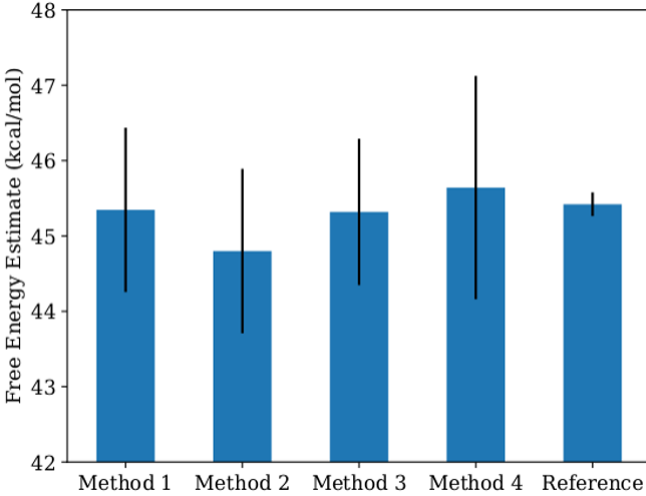


Fig. 7: Validation of expanded ensemble implementation: Observed variation of free energy estimate for implementations with one single simulation (Method 1), multiple simulations with no analysis (Method 2), local analysis (Method 3) and global analysis (Method 4). Error bars for each method represent the standard deviation of the MBAR estimates when data is not pooled between ensemble members. In the case of Method 1 the error is reported as the same error as Method 2. Reference free energy estimate is the MBAR estimate and standard deviation of four 200 ns fixed weight expanded-ensemble simulations.

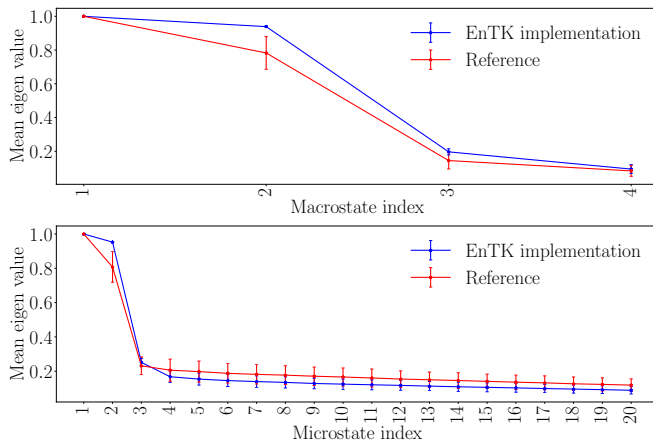


Fig. 8: Mean eigenvalue attained by the macro-states (top) and micro-states (bottom) by alanine dipeptide after aggregate simulation duration of 100ns implemented using EnTK compared against reference data

We compare the EnTK implementation against reference data from the msmbuilder package [74] by performing the clustering of the reference data and deriving the mean eigenvalues of the macro- and micro-states.

Eigen values attained by the macro-states (top) and micro-states (bottom) in the EnTK implementation and reference data are plotted as a function of the aggregate simulation in Figure 8. Final eigenvalues attained by the implementation agree with the reference data within the error bounds.

C. Expanded Ensemble at scale

We analyzed the convergence properties of the free energy estimate using the data generated for validation. MBAR was used to estimate the free energy difference of cucurbit[7]uril

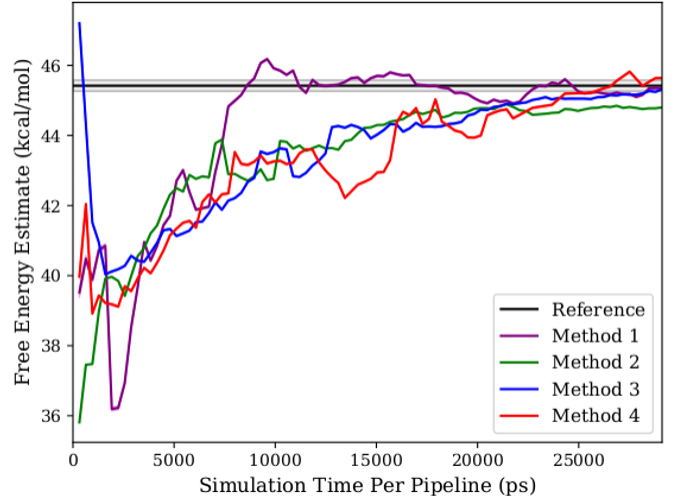


Fig. 9: Convergence of expanded ensemble implementation: Observed convergence behavior of free energy estimate for implementations with one single simulation (Method 1), multiple simulations with no analysis (Method 2), local analysis (Method 3) and global analysis (Method 4). Error bars for each method represent the MBAR standard error estimates. Reference free energy estimate is the MBAR estimate of the pooled data and the standard deviation of the non-pooled MBAR estimates of four 200 ns fixed weight expanded ensemble simulations.

(host) 6-amino-1-hexanol (guest) binding as a function of total simulation time available per ensemble member, using the latter 2/3 of the simulation data. This data is plotted for each method, as well as the reference calculation, in Figure 9. The convergence behavior of Method 1 observed in Figure 9 implies that the current method converges faster than ensemble based methods but does not represent the average behavior of the non-ensemble based approach. The average behavior is depicted more clearly by Method 2 because this method averages the free energy estimate of 16 independent single simulations.

The most significant feature of Figure 9 is that all three ensemble based methods converge at similar rates to the reference value. It was hypothesized that adding adaptive analysis to the estimate of the weights would improve convergence behavior but we see no significant change currently. Our initial hypothesis detailed that this would occur because the most probable configurations would be more likely to be generated in multiple pipelines, and sharing their weight information would bias other pipelines towards the most probable configurations. Our observation of the results, leads us to hypothesize instead that the most probable configurations are also being biased away by sharing weights from the other conformations in other ensemble members, leading to effectively no net improvement.

The results of the specific adaptive expanded ensemble method implemented here did not exhibit accelerated convergence rates. However, the methodology described here gives researchers the ability to implement additional adaptive elements and test their effects on system properties. Additionally, these adaptive elements can be implemented on relatively short time scales, giving the ability to test many implementations.

VII. SUMMARY

Scientific problems across domains such as biomolecular science, climate science and uncertainty quantification require multiple distinct computational tasks to be executed in order to achieve a desired solution. Novel approaches focus on leveraging intermediate data to adapt the application to study larger problems, longer time scales and to engineer better fidelity in the modeling of complex phenomena. In this paper, we described the operations in executing adaptive applications, classified the different types of application adaptivity, and described challenges in implementing them in software tools. We enhanced EnTK to support the execution of adaptive applications on HPC systems. We characterized the various overheads in the EnTK, validated the implementation of the two science drivers and executed EE at production scale and evaluated its sampling capabilities. To the best of our knowledge, this is the first that application adaptivity is studied in detail, and multiple adaptive ensemble applications have been implemented using a common conceptual and implementation framework.

REFERENCES

- [1] M. Turilli, F. F. Liu, Z. Zhang, A. Merzky, M. Wilde, J. Weissman, D. S. Katz, and S. Jha, "Integrating abstractions to enhance the execution of distributed applications," in *Proceedings of 30th IEEE International Parallel and Distributed Processing Symposium (IPDPS)*, 2016 (in press), <http://arxiv.org/abs/1504.04720>.
- [2] D. E. Shaw, M. M. Deneroff, R. O. Dror, J. S. Kuskin, R. H. Larson, J. K. Salmon, C. Young, B. Batson, K. J. Bowers, J. C. Chao *et al.*, "Anton, a special-purpose machine for molecular dynamics simulation," *Communications of the ACM*, vol. 51, no. 7, pp. 91–97, 2008.
- [3] Y. Komeiji, M. Uebayasi, R. Takata, A. Shimizu, K. Itsukashi, and M. Taiji, "Fast and accurate molecular dynamics simulation of a protein using a special-purpose computer," *Journal of Computational Chemistry*, vol. 18, no. 12, pp. 1546–1563, 1997.
- [4] S. Trebst, M. Troyer, and U. H. Hansmann, "Optimized parallel tempering simulations of proteins," *The Journal of chemical physics*, vol. 124, no. 17, p. 174903, 2006.
- [5] A. Mitsutake and Y. Okamoto, "Replica-exchange extensions of simulated tempering method," *The Journal of chemical physics*, vol. 121, no. 6, pp. 2491–2504, 2004.
- [6] J. Comer, J. C. Phillips, K. Schulten, and C. Chipot, "Multiple-replica strategies for free-energy calculations in namd: multiple-walker adaptive biasing force and walker selection rules," *Journal of chemical theory and computation*, vol. 10, no. 12, pp. 5276–5285, 2014.
- [7] S. Rauscher, C. Neale, and R. Pomes, "Simulated tempering, distributed replica sampling, virtual replica exchange, and other generalized-ensemble methods for conformational sampling," *Journal of chemical theory and computation*, vol. 5, no. 10, pp. 2640–2662, 2009.
- [8] E. Vanden-Eijnden and M. Venturoli, "Markovian milestoning with voronoi tessellations," *The Journal of chemical physics*, vol. 130, no. 19, p. 194101, 2009.
- [9] A. K. Faradjian and R. Elber, "Computing time scales from reaction coordinates by milestoning," *The Journal of chemical physics*, vol. 120, no. 23, pp. 10 880–10 889, 2004.
- [10] L. Maragliano, B. Roux, and E. Vanden-Eijnden, "Comparison between mean forces and swarms-of-trajectories string methods," *Journal of chemical theory and computation*, vol. 10, no. 2, pp. 524–533, 2014.
- [11] A. Atzori, N. J. Bruce, K. K. Burusco, B. Wroblowski, P. Bonnet, and R. A. Bryce, "Exploring protein kinase conformation using swarm-enhanced sampling molecular dynamics," *Journal of chemical information and modeling*, vol. 54, no. 10, pp. 2764–2775, 2014.
- [12] J. D. Chodera, W. C. Swope, J. W. Pitera, and K. A. Dill, "Long-time protein folding dynamics from short-time molecular dynamics simulations," *Multiscale Modeling & Simulation*, vol. 5, no. 4, pp. 1214–1226, 2006.
- [13] G. R. Bowman, X. Huang, and V. S. Pande, "Using generalized ensemble simulations and markov state models to identify conformational states," *Methods*, vol. 49, no. 2, pp. 197–201, 2009.
- [14] D. A. Case, T. E. Cheatham, T. Darden, H. Gohlke, R. Luo, K. M. Merz, A. Onufriev, C. Simmerling, B. Wang, and R. J. Woods, "The amber biomolecular simulation programs," *Journal of computational chemistry*, vol. 26, no. 16, pp. 1668–1688, 2005.
- [15] M. J. Abraham, T. Murtola, R. Schulz, S. Páll, J. C. Smith, B. Hess, and E. Lindahl, "Gromacs: High performance molecular simulations through multi-level parallelism from laptops to supercomputers," *SoftwareX*, vol. 1, pp. 19–25, 2015.
- [16] J. C. Phillips, R. Braun, W. Wang, J. Gumbart, E. Tajkhorshid, E. Villa, C. Chipot, R. D. Skeel, L. Kale, and K. Schulten, "Scalable molecular dynamics with namd," *Journal of computational chemistry*, vol. 26, no. 16, pp. 1781–1802, 2005.
- [17] W. Jiang, J. C. Phillips, L. Huang, M. Fajer, Y. Meng, J. C. Gumbart, Y. Luo, K. Schulten, and B. Roux, "Generalized scalable multiple copy algorithms for molecular dynamics simulations in namd," *Computer physics communications*, vol. 185, no. 3, pp. 908–916, 2014.
- [18] M. Bonomi, D. Branduardi, G. Bussi, C. Camilloni, D. Provasi, P. Raiteri, D. Donadio, F. Marinelli, F. Pietrucci, R. A. Broglia *et al.*, "Plumed: A portable plugin for free-energy calculations with molecular dynamics," *Computer Physics Communications*, vol. 180, no. 10, pp. 1961–1972, 2009.
- [19] G. Hummer and I. G. Kevrekidis, "Coarse molecular dynamics of a peptide fragment: Free energy, kinetics, and long-time dynamics computations," *The Journal of chemical physics*, vol. 118, no. 23, pp. 10 762–10 773, 2003.
- [20] H. Grubmüller, "Predicting slow structural transitions in macromolecular systems: Conformational flooding," *Physical Review E*, vol. 52, no. 3, p. 2893, 1995.
- [21] M. Stonebraker, "Too much middleware," *ACM Sigmod Record*, vol. 31, no. 1, pp. 97–106, 2002.
- [22] R. A. Van Engelen and K. A. Gallivan, "The gsoap toolkit for web services and peer-to-peer computing networks," in *Cluster Computing and the Grid, 2002. 2nd IEEE/ACM International Symposium on*. IEEE, 2002, pp. 128–128.
- [23] Y. Tanaka, H. Nakada, S. Sekiguchi, T. Suzumura, and S. Matsuoka, "Ninf-g: A reference implementation of rpc-based programming middleware for grid computing," *Journal of Grid computing*, vol. 1, no. 1, pp. 41–51, 2003.
- [24] M. Sato, T. Boku, and D. Takahashi, "Omnirpc: a grid rpc system for parallel programming in cluster and grid environment," in *Cluster Computing and the Grid, 2003. Proceedings. CCGrid 2003. 3rd IEEE/ACM International Symposium on*. IEEE, 2003, pp. 206–213.
- [25] M. Mattoso, J. Dias, K. A. Ocaña, E. Ogasawara, F. Costa, F. Horta, V. Silva, and D. de Oliveira, "Dynamic steering of hpc scientific workflows: A survey," *Future Generation Computer Systems*, vol. 46, pp. 100–113, 2015.
- [26] S. Bowers, B. Ludascher, A. H. Ngu, and T. Critchlow, "Enabling scientific workflow reuse through structured composition of dataflow and control-flow," in *Data engineering workshops, 2006. proceedings. 22nd international conference on*. IEEE, 2006, pp. 70–70.
- [27] B. Ludäscher, I. Altintas, C. Berkley, D. Higgins, E. Jaeger, M. Jones, E. A. Lee, J. Tao, and Y. Zhao, "Scientific workflow management and the kepler system," *Concurrency and Computation: Practice and Experience*, vol. 18, no. 10, pp. 1039–1065, 2006.
- [28] P. Missier, S. Soland-Reyes, S. Owen, W. Tan, A. Nenadic, I. Dunlop, A. Williams, T. Oinn, and C. Goble, "Taverna, reloaded," in *International conference on scientific and statistical database management*. Springer, 2010, pp. 471–481.
- [29] E. Deelman, G. Singh, M.-H. Su, J. Blythe, Y. Gil, C. Kesselman, G. Mehta, K. Vahi, G. B. Bertram, J. Good *et al.*, "Pegasus: A framework for mapping complex scientific workflows onto distributed systems," *Scientific Programming*, vol. 13, no. 3, pp. 219–237, 2005.
- [30] T. Samak, D. Gunter, M. Goode, E. Deelman, G. Mehta, F. Silva, and K. Vahi, "Failure prediction and localization in large scientific workflows," in *Proceedings of the 6th workshop on Workflows in support of large-scale science*. ACM, 2011, pp. 107–116.
- [31] S. Pronk, I. Pouya, M. Lundborg, G. Rotskoff, B. Wesen, P. M. Kasson, and E. Lindahl, "Molecular simulation workflows as parallel algorithms: The execution engine of copernicus, a distributed high-performance computing platform," *Journal of chemical theory and computation*, vol. 11, no. 6, pp. 2600–2608, 2015.
- [32] P. K. McKinley, S. M. Sadjadi, E. P. Kasten, and B. H. Cheng, "Composing adaptive software," *Computer*, vol. 37, no. 7, pp. 56–64, 2004.
- [33] A. Laio and M. Parrinello, "Escaping free-energy minima," *Proc. Natl. Acad. Sci. USA*, vol. 99, no. 20, Oct. 2002.
- [34] M. Bonomi, D. Branduardi, G. Bussi, C. Camilloni, D. Provasi, P. Raiteri, D. Donadio, F. Marinelli, F. Pietrucci, R. A. Broglia, and M. Parrinello, "PLUMED: A portable plugin for free-energy calculations with molecular dynamics," *Comput. Phys. Commun.*, vol. 180, no. 10, pp. 1961–1972, Oct. 2009. [Online]. Available: [http://www.sciencedirect.com/science?_ob=ArticleURL&_udi=B6TJ5-4W91PWV-7&_user=709071&_rdoc=1&_fmt=&_orig=search&_sort=d&_docanchor=&view=c&_acct=C000039638&_v](http://www.sciencedirect.com/science/article/B6TJ5-4W91PWV-7/2/4b543dff25a51c136ac931316269ef0http://www.sciencedirect.com/science?_ob=ArticleURL&_udi=B6TJ5-4W91PWV-7&_user=709071&_rdoc=1&_fmt=&_orig=search&_sort=d&_docanchor=&view=c&_acct=C000039638&_v)
- [35] A. Barducci, M. Bonomi, and M. Parrinello, "Metadynamics," *Wiley Interdiscip. Rev. Comput. Mol. Sci.*, vol. 1, no. 5, pp. 826–843, Sep. 2011. [Online]. Available: <http://doi.wiley.com/10.1002/wcms.31>
- [36] W. Nadler and U. H. E. Hansmann, "Generalized ensemble and tempering simulations: A unified view," *Phys. Rev. E*, vol. 75, p. 026109, 2007.
- [37] S. Park and V. S. Pande, "Choosing weights for simulated tempering," *Phys. Rev. E*, vol. 76, p. 016703, 2007.
- [38] A. P. Lyubartsev, A. A. Martsinovski, S. V. Shevkunov, and P. N. Vorontsov-Velyaminov, "New approach to Monte Carlo calculation of the free energy: Method of expanded ensembles," *J. Chem. Phys.*, vol. 96, no. 3, p. 1776, Feb. 1992. [Online]. Available: <http://scitation.aip.org/content/aip/journal/jcp/96/3/10.1063/1.462133>
- [39] Y. Iba, "Extended ensemble monte carlo," *Int. J. Mod. Phys. C-Physics Comput.*, vol. 12, no. 5, pp. 623–656, 2001.

[40] R. Chelli and G. F. Signorini, "Serial Generalized Ensemble Simulations of Biomolecules with Self-Consistent Determination of Weights," *J. Chem. Theory Comput.*, vol. 8, no. 3, pp. 830–842, Mar. 2012. [Online]. Available: <http://dx.doi.org/10.1021/ct2008457>

[41] J. D. Chodera and M. R. Shirts, "Replica exchange and expanded ensemble simulations as Gibbs sampling: simple improvements for enhanced mixing," *J. Chem. Phys.*, vol. 135, no. 19, p. 194110, Nov. 2011. [Online]. Available: <http://scitation.aip.org/content/aip/journal/jcp/135/19/10.1063/1.3660669>

[42] M. K. Fenwick and F. A. Escobedo, "Expanded ensemble and replica exchange methods for simulation of protein-like systems," *J. Chem. Phys.*, vol. 119, no. 22, pp. 11 998–12 010, 2003.

[43] S. Park, "Comparison of the serial and parallel algorithms of generalized ensemble simulations: An analytical approach," *Phys. Rev. E*, vol. 77, p. 016709, 2008.

[44] J. Ferklinghoff-Borg, "Optimized Monte Carlo analysis for generalized ensembles," *Eur. Phys. J. B-Condensed Matter Complex Syst.*, vol. 29, no. 3, pp. 481–484, 2002.

[45] J. Comer, J. C. Phillips, K. Schulten, and C. Chipot, "Multiple-Replica Strategies for Free-Energy Calculations in NAMD: Multiple-Walker Adaptive Biasing Force and Walker Selection Rules," *J. Chem. Theory Comput.*, vol. 10, no. 12, pp. 5276–5285, Dec. 2014. [Online]. Available: <http://dx.doi.org/10.1021/ct500874p>

[46] L. Janosi and M. Doxastakis, "Accelerating flat-histogram methods for potential of mean force calculations," *J. Chem. Phys.*, vol. 131, no. 5, p. 054105, Aug. 2009. [Online]. Available: <http://scitation.aip.org/content/aip/journal/jcp/131/5/10.1063/1.3183165>

[47] P. Raiteri, A. Laiò, F. L. Gervasio, C. Micheletti, and M. Parrinello, "Efficient reconstruction of complex free energy landscapes by multiple walkers metadynamics," *J. Phys. Chem. B*, vol. 110, pp. 3533–3539, 2006.

[48] N. Singhal and V. S. Pande, "Error analysis and efficient sampling in markovian state models for molecular dynamics," *The Journal of chemical physics*, vol. 123, no. 20, p. 204909, 2005.

[49] N. S. Hinrichs and V. S. Pande, "Calculation of the distribution of eigenvalues and eigenvectors in markovian state models for molecular dynamics," *The Journal of chemical physics*, vol. 126, no. 24, p. 244101, 2007.

[50] S. Trebst, M. Troyer, and U. H. E. Hansmann, "Optimized parallel tempering simulations of proteins," *J. Chem. Phys.*, vol. 124, p. 174903, 2006.

[51] U. H. E. Hansmann, "Parallel tempering algorithm for conformational studies of biological molecules," *Chem. Phys. Lett.*, vol. 281, pp. 140–150, 1997.

[52] A. Mitsutake, Y. Sugita, and Y. Okamoto, "Replica-exchange multicanonical and multicanonical replica-exchange monte carlo simulations of peptides. i. formulation and benchmark test," *The Journal of chemical physics*, vol. 118, no. 14, pp. 6664–6675, 2003.

[53] A. Mitsutake and Y. Okamoto, "Replica-exchange extensions of simulated tempering method," *J. Chem. Phys.*, vol. 121, p. 2491, 2004.

[54] A. J. Ballard and C. Jarzynski, "Replica exchange with nonequilibrium switches," *Proc. Natl. Acad. Sci.*, vol. 106, no. 30, pp. 12 224–12 229, Jul. 2009. [Online]. Available: <http://www.pnas.org/content/106/30/12224>

[55] S. Rauscher, C. Neale, and R. Pomes, "Simulated Tempering Distributed Replica Sampling, Virtual Replica Exchange, and Other Generalized-Ensemble Methods for Conformational Sampling," *J. Chem. Theory Comput.*, vol. 5, no. 10, pp. 2640–2662, Oct. 2009. [Online]. Available: <http://dx.doi.org/10.1021/ct900302n>

[56] B. K. Radak, M. Romanus, T.-S. Lee, H. Chen, M. Huang, A. Treikalis, V. Balasubramanian, S. Jha, and D. M. York, "Characterization of the Three-Dimensional Free Energy Manifold for the Uracil Ribonucleoside from Asynchronous Replica Exchange Simulations," *J. Chem. Theory Comput.*, vol. 11, no. 2, pp. 373–377, Jan. 2015. [Online]. Available: <http://dx.doi.org/10.1021/ct500776j>

[57] R. Affentranger, I. Tavernelli, and E. E. Di Iorio, "A Novel Hamiltonian Replica Exchange MD Protocol to Enhance Protein Conformational Space Sampling," *J. Chem. Theory Comput.*, vol. 2, no. 2, pp. 217–228, Mar. 2006. [Online]. Available: <http://dx.doi.org/10.1021/ct050250b>

[58] A. Shmygelska and M. Levitt, "Generalized ensemble methods for de novo structure prediction," *Proc. Natl. Acad. Sci.*, vol. 106, no. 5, pp. 1415–1420, Feb. 2009. [Online]. Available: <http://www.pnas.org/content/106/5/1415.abstract>

[59] K. Wang, J. D. Chodera, Y. Yang, and M. R. Shirts, "Identifying ligand binding sites and poses using GPU-accelerated Hamiltonian replica exchange molecular dynamics," *J. Comput. Aided. Mol. Des.*, vol. 27, no. 12, pp. 989–1007, Dec. 2013. [Online]. Available: <http://www.ncbi.nlm.nih.gov/pubmed/24297454>

[60] W. M. van der Aals and S. Jablonski, "Dealing with workflow change: identification of issues and solutions," *Computer systems science and engineering*, vol. 15, no. 5, pp. 267–276, 2000.

[61] V. Balasubramanian, A. Treikalis, O. Weidner, and S. Jha, "Ensemble Toolkit: Scalable and Flexible Execution of Ensembles of Tasks," in *Proceedings of the 45th International Conference on Parallel Processing (ICPP)*, 2016, <http://arxiv.org/abs/1602.00678>.

[62] V. Balasubramanian, M. Turilli, W. Hu, M. Lefebvre, W. Lei, G. Cervone, J. Tromp, and S. Jha, "Harnessing the power of many: Extensible toolkit for scalable ensemble applications," 2018, <https://arxiv.org/abs/1710.08491>.

[63] "Rabbitmq," <https://www.rabbitmq.com/> (accessed March 2018).

[64] A. Merzky, M. Santcroos, M. Turilli, and S. Jha, "Executing Dynamic and Heterogeneous Workloads on Super Computers," 2016, (under review) <http://arxiv.org/abs/1512.08194>.

[65] A. Merzky, M. Turilli, M. Maldonado, M. Santcroos, and S. Jha, "Using pilot systems to execute many task workloads on supercomputers," 2018, (under review) <http://arxiv.org/abs/1512.08194>.

[66] "Msmbuilder," <https://github.com/msmbuilder/msmbuilder> (accessed March 2018).

[67] "Md trajectories of ala2," https://figshare.com/articles/new_fileset/1026131 (accessed March 2018).

[68] "Stress-ng," <http://kernel.ubuntu.com/~cking/stress-ng/stress-ng.pdf> (accessed March 2018).

[69] S. Pronk, S. Pál, R. Schulz, P. Larsson, P. Bjelkmar, R. Apostolov, M. R. Shirts, J. C. Smith, P. M. Kasson, D. Van Der Spoel *et al.*, "Gromacs 4.5: a high-throughput and highly parallel open source molecular simulation toolkit," *Bioinformatics*, vol. 29, no. 7, pp. 845–854, 2013.

[70] "Openmm," <https://github.com/pandegroup/openmm> (accessed March 2018).

[71] "Lsu supermic," <https://portal.xsede.org/lwu-supermic> (accessed March 2018).

[72] F. Wang and D. P. Landau, "Efficient, multiple-range random walk algorithm to calculate density of states," *Phys. Rev. Lett.*, vol. 86, pp. 2050–2053, 2001.

[73] M. R. Shirts and J. D. Chodera, "Statistically optimal analysis of samples from multiple equilibrium states," *J. Chem. Phys.*, vol. 129, p. 124105, 2008.

[74] "Md trajectories of ala2," https://figshare.com/articles/new_fileset/1026131 (accessed March 2018).

APPENDIX A

ARTIFACT DESCRIPTION APPENDIX: IMPLEMENTING ADAPTIVE BIOMOLECULAR APPLICATIONS AT SCALE

A. Abstract

This artifact contains information to enable the reproduction of results presented in our SC'18 paper titled “Implementing Adaptive Biomolecular Applications at Scale”. The source code, data, and post analysis scripts for our experiments are available publicly on Github while the raw data from the experiments is made available via Google drive URLs. We also document instructions to install our tools and execute all our scripts on the same HPC systems as in our experiments

B. Description

1) *Check-list (artifact meta information): Fill in whatever is applicable with some informal keywords and remove the rest*

- **Algorithm:** Expanded Ensemble and Markov State Model based molecular dynamics
- **Program:** Gromacs, Alchemical analysis, Ensemble Toolkit
- **Compilation:** Gromacs and Alchemical analysis were compiled on the XSEDE SuperMIC machine
- **Binary:** Gromacs and python
- **Data set:** Available on public Github repo
- **Run-time environment:** XSEDE SuperMIC for Gromacs and Ubuntu 16.04.4 LTS (GNU/Linux 4.4.047generic x86_64) for Ensemble Toolkit
- **Hardware:** All simulations and analysis were run on XSEDE SuperMIC, Ensemble Toolkit was installed on a VM with Intel(R) Core(TM) i7 6700 CPU and 64GB RAM
- **Output:** MD data generated on XSEDE SuperMIC, profiling data generated on VM; also made available via Google Drive
- **Experiment workflow:** Install EnTK and execute python file under ‘bin’ in each experiment folder on Github repo
- **Publicly available?:** Yes

2) *How software can be obtained (if available):*

3) *Hardware dependencies:* All scripts are configured to execute on XSEDE SuperMIC alone

4) *Software dependencies:* The required versions of Gromacs, OpenMM, and alchemical analysis are installed on SuperMIC and made public. We describe the general installation instructions for any resource below. Documentation regarding installation of EnTK and its dependencies are available at <http://radicalentk.readthedocs.io/en/latest/>.

5) *Datasets:* The datasets and scripts required for each experiment are available at <https://github.com/radical-experiments/adaptive-bms-experiments> under the following folders.

- Task count adaptivity - i task-count-adap/bin
- Task order adaptivity - i task-order-adap/bin
- Task attribute adaptivity - i task-attribute-adap/bin
- Expanded ensemble - i expanded-ensemble-experiments/;method index i /bin
- MSM - i adaptive-msm-validation/bin

C. Installation

Gromacs, OpenMM and alchemical analysis are installed on SuperMIC and made publicly accessible. EnTK is required to be installed on a machine that has persistent, password-less ssh/gsish access to SuperMIC. We mention below the

installation instructions that might be helpful to install on other machines.

1) *Gromacs:* Clone GROMACS 5.1.3 with Wang-Landau modification and compile as follows

```
$ git clone https://github.com/shirtsgroup/gromacs_wlmod/
  tree/5.1.3
$ cd gromacs_wlmod
$ mkdir build
$ cd build
$ cmake .. -DGMX_BUILD_OWN_FFTW=ON -
  DREGRESSIONTEST_DOWNLOAD=ON
$ make
$ make check
```

2) *OpenMM:* OpenMM can be directly installed from the anaconda distribution.

```
$ conda install -c omnia openmm
```

3) *Alchemical analysis:* Clone Alchemical Analysis and install

```
$ git clone https://github.com/MobleyLab/alchemical-
  analysis.git
$ cd alchemical-analysis
$ sudo python setup.py install
```

4) *EnTK:* EnTK is published in the pypi repository and can be installed directly in a virtualenv.

```
$ virtualenv $HOME/myenv
$ $source $HOME/myenv/bin/activate
$ pip install radical.entk
```

D. Experiment workflow

Before running any of the scripts, you will be required to have password-less access to SuperMIC. Instructions on setting up such a configuration is available at <http://radicalentk.readthedocs.io/en/latest/install.html#setup-passwordless-ssh-access-to-machines> or can be found by searching the web.

Clone the repository at <https://github.com/radical-experiments/adaptive-bms-experiments> to get the scripts and data for all the experiments. Depending on the experiment, traverse the repository to the appropriate folder as specified in the datasets field of the appendix. Follow the execution command on the README of that folder to perform the experiments.

E. Evaluation and expected result

In the case of characterization experiments, multiple profiles are generated on the user machine which need to be analyzed to produce plots similar to the ones in our paper. In the case of experiments with MSM and EE, trajectory data is generated which is to be analyzed. Jupyter notebooks are made available in the same repository as the datasets under <experiment name>/notebook folder with instructions for running the notebook.

F. Experiment customization

The executable scripts provided in the datasets assumes that the target resource is SuperMIC and the user intends to use the tools installed by the authors.

Changes to the tools require appropriate changes in the environment settings for each task. This requires changing the *pre_exec* attributes in the executable scripts. Changes to the

target resource requires update to the resource description in the *res_dict* dictionary in each executable script.

G. Notes

- EnTK is needs to be installed on client machine which has persistent, password-less access to the target HPC system